

Focused Heating in Cylindrical Targets: Part I

JAMES R. WAIT, FELLOW, IEEE

Abstract — The analytical basis of a method to focus the electromagnetic power into a conductive cylinder is described. The scheme, as currently being used by others, is to locate a number of horn apertures around the periphery. An explicit expression is obtained for the required excitation of the apertures for a two-dimensional model.

I. INTRODUCTION

A need exists to localize the power deposition in human limbs and torsos in cancer therapy. Various applicators in the forms of loops and horn antennas have been used in selected configurations [1]–[6]. The common objective has been to heat the tumor while minimizing the damage to the adjacent healthy tissue. By persistent experimentation, several schemes have been developed that appear to be effective. On the theoretical side, the effort has been directed to both analytical and numerical modeling using idealized model shapes. With a few notable exceptions (e.g., [5]), the approaches have been rather empirical in that the source configurations and manner of excitation are assumed rather than deduced from the desired pattern of the power deposition in the target.

Our purpose here is to outline a procedure for focusing the power deposited in a lossy body of cylindrical form using an array of aperture antennas. For purposes of illustration, we adopt a two-dimensional cylindrical model. In Part II, we will consider numerical results and specific examples.

II. THE MODEL

The cylindrical configuration is shown in Fig. 1. The biological target (i.e., torso or limb) is represented by a homogeneous cylinder of radius a with conductivity σ_1 and permittivity ϵ_1 . With respect to a cylindrical coordinate system (ρ, ϕ, z) , the surface of the target is $\rho = a$ for $-\infty < z < +\infty$. At the concentric cylindrical surface $\rho = b$, we now apply an aperture electric field $E_z(\rho, \phi)$ polarized in the z -direction. As indicated below, this aperture illumination is to be implemented by a finite number N of horn antennas (in Fig. 1, $N = 8$). The annular region $a < \rho < b$ is homogeneous with assigned conductivity σ_2 and permittivity ϵ_2 . This region can be either free space ($\sigma_2 = 0, \epsilon_2 = \epsilon_0$) or de-ionized water ($\sigma_2 \approx 0, \epsilon_2 \approx 81\epsilon_0$). In this study, we do not consider the TE (transverse electric) polarization because of difficulties in practical implementation.

III. ANALYSIS

Our first task is to obtain an expression for the electric field $E_z(\rho, \phi)$ at any interior point (i.e., $\rho < b$), in terms of the aperture field $E_z(b, \phi)$. We deal with harmonic time dependence of the form $\exp(i\omega t)$, where ω is the angular frequency. Because the fields satisfy Maxwell's equation and remembering that $\partial/\partial z = 0$, it is a simple matter to show that

$$(\nabla^2 - \gamma^2) E_z(\rho, \phi) = 0 \quad (1)$$

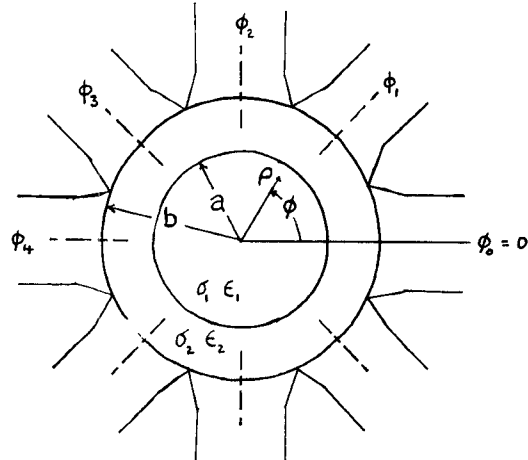


Fig. 1. Plan view of general scheme showing location of horn aperture antennas around cylindrical target of radius a with buffer zone of outer radius b .

where

$$\nabla^2 = \frac{1}{\rho} \frac{\partial}{\partial \rho} \rho \frac{\partial}{\partial \rho} + \frac{1}{\rho^2} \frac{\partial^2}{\partial \phi^2} \quad (2)$$

is the Laplacian operator, and

$$\gamma = [i\mu_0\omega(\sigma + i\epsilon\omega)]^{1/2} \quad (3)$$

is the complex propagation constant. We add a subscript 1 or 2 to γ , σ , and ϵ as appropriate. Here, μ_0 is the magnetic permeability that we assume is the free-space value $4\pi \times 10^{-7}$ throughout. The corresponding magnetic-field components are then obtained from

$$H_\rho = -\frac{1}{i\mu_0\omega} \frac{\partial E_z}{\rho \partial \phi} \quad (4)$$

and

$$H_\phi = \frac{1}{i\mu_0\omega} \frac{\partial E_z}{\partial \rho}. \quad (5)$$

Appropriate forms of the solutions [7], [8] for E_z and H_ϕ in the various regions are given below. For $0 < \rho < a$, we have

$$E_z = \sum_{m=-\infty}^{+\infty} A_m I_m(\gamma_1 \rho) e^{-im\phi} \quad (6)$$

and

$$H_\phi = y_1 \sum_{m=-\infty}^{+\infty} A_m I'_m(\gamma_1 \rho) e^{-im\phi} \quad (7)$$

where $I_m(Z)$ is the modified Bessel function [9] of argument Z and $I'_m(Z) = dI_m(Z)/dZ$ and where $y_1 = \gamma_1/(i\mu_0\omega) = [(\sigma_1 + i\epsilon_1\omega)/(i\mu_0\omega)]^{1/2}$ is the intrinsic admittance of the target region. A_m is a coefficient yet to be determined.

For $a < \rho < b$, we have

$$E_z = \sum_{m=-\infty}^{+\infty} [B_m I_m(\gamma_2 \rho) + C_m K_m(\gamma_2 \rho)] e^{-im\phi} \quad (8)$$

and

$$H_\phi = y_2 \sum_{m=-\infty}^{+\infty} [B_m I'_m(\gamma_2 \rho) + C_m K'_m(\gamma_2 \rho)] e^{-im\phi} \quad (9)$$

where $K_m(Z)$ is the MacDonald function [9] of argument Z and $K'_m(Z) = dK_m(Z)/dZ$ and where $y_2 = \gamma_2/(i\mu_0\omega) = [(\sigma_2 + i\epsilon_2\omega)/(i\mu_0\omega)]^{1/2}$.

Manuscript received October 30, 1984; revised February 15, 1985.
The author is with the Electrical Engineering Department, University of Arizona, Tucson, AZ 85721.

$i\epsilon_2\omega)/(i\mu_0\omega)]^{1/2}$ is the intrinsic admittance of the buffer region. B_m and C_m are coefficients yet to be determined.

The boundary conditions at $\rho = a$ (i.e., surface of the target) require that E_z and H_ϕ are continuous. Application to (6)–(9) lead to the following relations:

$$C_m = B_m R_m \quad (10)$$

where

$$R_m = - \left[\frac{y_2 I'_m(\gamma_2 a) - Y_{1,m} I_m(\gamma_2 a)}{y_2 K'_m(\gamma_2 a) - Y_{1,m} K_m(\gamma_2 a)} \right] \quad (11)$$

where

$$Y_{1,m} = y_1 I'_m(\gamma_1 a) / I_m(\gamma_1 a) \quad (12)$$

and also

$$A_m = B_m [I_m(\gamma_2 a) + R_m K_m(\gamma_2 a)] / I_m(\gamma_1 a). \quad (13)$$

The remaining unknown coefficient B_m is determined by the aperture field at $\rho = b$. For example, we can write

$$E_z(b, \phi) = \sum_{m=-\infty}^{+\infty} E_m e^{-im\phi} \quad (14)$$

provided the Fourier transform

$$E_m = \frac{1}{2\pi} \int_0^{2\pi} E_z(b, \phi) e^{im\phi} d\phi \quad (15)$$

exists. On using (8) and (10) for the left-hand side of (14), it follows that

$$B_m [I_m(\gamma_2 b) + R_m K_m(\gamma_2 b)] = E_m \quad (16)$$

which is the desired relation between B_m and E_m .

Now clearly if the aperture field (14) is specified at the outset, we may use (16) and (13) to yield the coefficient A_m for the field inside the target. To be explicit

$$A_m = f_m E_m \quad (17)$$

where

$$f_m = \frac{I_m(\gamma_2 a) + R_m K_m(\gamma_2 a)}{I_m(\gamma_1 a) [I_m(\gamma_2 b) + R_m K_m(\gamma_2 b)]}. \quad (18)$$

Thus, on using (6), the field inside the target (i.e., $\rho < a$) is expressed in the form

$$E_z(\rho, \phi) = \sum_{m=-\infty}^{+\infty} f_m E_m I_m(\gamma_1 \rho) e^{-im\phi} \quad (19)$$

where E_m is the Fourier transform of the aperture field. The corresponding magnetic-field components H_ρ and H_ϕ are obtained from (4) and (5), respectively.

IV. SYNTHESIS

In a formal sense, we may carry out a synthesis by starting with the premise that the internal field E_z at some fixed value of ρ ($= \rho_0$) is a prescribed function of ϕ . Then we wish to deduce the aperture field at $\rho = b$ that is required. In other words, let us say that

$$E_z(\rho_0, \phi) = g(\phi) \quad (20)$$

where $g(\phi)$ is specified. Then, in accordance with (19)

$$g(\phi) = \sum_{m=-\infty}^{+\infty} f_m E_m I_m(\gamma_1 \rho_0) e^{-im\phi} \quad (21)$$

that is to hold for $0 < \phi < 2\pi$. Then, by Fourier inversion of (21),

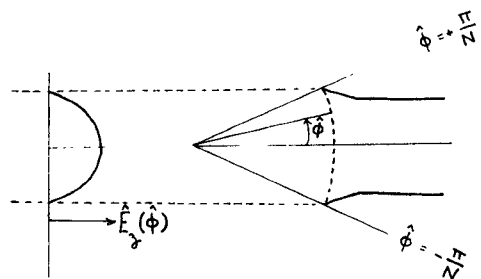


Fig. 2. Geometry for individual aperture of angular width $2\pi/N$ radians and sketch (to the left) of assumed aperture distribution of electric field.

we have

$$E_m = \frac{1}{f_m I_m(\gamma_1 \rho_0)} \frac{1}{2\pi} \int_0^{2\pi} g(\phi) e^{im\phi} d\phi \quad (22)$$

and the corresponding form for $E_z(b, \phi)$ is given by (14). Such a synthesis in terms of the desired ϕ variation is probably of limited value but it is possible the inverse property could be exploited at a later date.

V. FOCUSING

A more promising approach to the synthesis problem is to accept the limited goal of tailoring the aperture field to achieve focusing at some internal point (ρ, ϕ) where $\rho < a$. To this end, we actually break the aperture into N discrete segments such as depicted in Fig. 1 (where $N = 8$). We can envisage an individual segment as a horn aperture [3]. Thus, we see that

$$E_m = \frac{1}{2\pi} \int_0^{2\pi} E_z(b, \phi) e^{im\phi} d\phi = \sum_{n=0}^{N-1} E_{m,n} \quad (23)$$

where

$$E_{m,n} = \frac{1}{2\pi} \int_{\phi_n - \pi/N}^{\phi_n + \pi/N} E_z(b, \phi) e^{im\phi} d\phi. \quad (24a)$$

By a simple change of variable, we may write

$$E_{m,n} = \frac{1}{2\pi} \int_{-\pi/N}^{\pi/N} E_z(b, \phi_n + \hat{\phi}) e^{im(\phi_n + \hat{\phi})} d\hat{\phi}. \quad (24b)$$

Here $\hat{\phi} = \phi - \phi_n$ is the angular distance measured across an individual horn aperture. We now assume the following distribution of field is the n th horn:

$$E_z(b, \phi_n + \hat{\phi}) = \hat{E}_z(\hat{\phi}) \Delta_n e^{i\delta_n} \quad (25)$$

where Δ_n and δ_n are real. In other words, we are saying that the field distribution $\hat{E}_z(\hat{\phi})$ is the same in each horn but the magnitude and phase differ for each horn. The situation for an individual horn is depicted in Fig. 2. Now we see that

$$E_{m,n} = \frac{1}{2\pi b} \Delta_n e^{i\delta_n} e^{im\phi_n} V_m \quad (26)$$

where

$$V_m = b \int_{-\pi/N}^{\pi/N} \hat{E}_z(\hat{\phi}) e^{im\hat{\phi}} d\hat{\phi}. \quad (27)$$

We are now in the position to write (19) in the form

$$E_z(\rho, \phi) = \sum_{n=0}^{N-1} E_{z,n}(\rho, \phi) \quad (28)$$

where

$$E_{z,n}(\rho, \phi) = \frac{1}{2\pi b} \Delta_n e^{i\delta_n} \sum_{m=-\infty}^{+\infty} f_m V_m I_m(\gamma_1 \rho) e^{-im(\phi - \phi_n)} \quad (29)$$

can be identified as the contribution of the n th aperture to the field at (ρ, ϕ) . We can say that the array of N horn apertures is focused to the point (ρ, ϕ) when the phase of each contribution $E_{z,n}$ is identical. An equivalent statement is that

$$\delta_n = -\text{phase of } \sum_{m=-\infty}^{+\infty} f_m V_m I_m(\gamma_1 \rho) e^{-im(\phi-\phi_n)}. \quad (30)$$

The choice of the amplitude factor Δ_n is still open. The coefficient f_m is defined by (18) and involves the electrical properties of the target and the concentric buffer region. In the case where the latter is absent or vanishing small (i.e., $b \rightarrow a$), we see that

$$f_m = [I_m(\gamma_1 a)]^{-1}. \quad (31)$$

The other key coefficient in (30) is V_m , which depends on the common field distribution in a given aperture. Assuming that the horns are excited only by a TEM (transverse electromagnetic) mode, it is reasonable to assume a sinusoidal field distribution at the aperture which vanishes at the side walls. Thus, we may adopt the form

$$\hat{E}_z(\hat{\phi}) = E_0 \cdot \cos\left(\frac{N\hat{\phi}}{2}\right) \quad (32)$$

for the range $-\frac{\pi}{N} < \hat{\phi} < \frac{\pi}{N}$. Then, using (27), we see that

$$\begin{aligned} V_m &= bE_0 \int_{-\pi N}^{\pi N} \cos\left(\frac{N\hat{\phi}}{2}\right) e^{im\hat{\phi}} d\hat{\phi} \\ &= bE_0 \cos\left(m \frac{\pi}{N}\right) \frac{N}{(N/2)^2 - m^2} \\ &= bE_0 \pi/N \quad \text{for } m = N/2. \end{aligned} \quad (33)$$

All quantities on the right-hand side of (30) are now specified, and the phase factors δ_n may be calculated for any desired point (ρ, ϕ) . We are still free to select the amplitude factors Δ_n if additional constraints are made.

VI. FINAL REMARKS

There are a number of generalizations and extensions of the present model that we might mention. The case where the target (defined by $\rho < a$ in Fig. 1) is concentrically layered presents no difficulty in analysis. Here, we can use the present formulation provided $Y_{1,m}$ (the surface admittance) of mode of order m at $\rho = a$ is replaced by the appropriate form for the equivalent nonuniform transmission line [8]. Another extension is to allow explicitly for the limited axial extent (in the z -direction) of the apertures and to include the axial variation of the fields [8],[10]. Now we must allow for the intrinsic hybrid nature of the fields because the TE (transverse electric) and TM (transverse magnetic) modes are coupled [8]. At the same time, both the axial and the azimuthal (i.e., z and ϕ , respectively) variations of the aperture fields can be accounted for. In a further extension, we can consider the influence of the finite length of the cylindrical target by imposing a zero axial current flow condition at the bounding planes (top and bottom) [11].

There is another interesting concept that we might also mention in the present context. In order to "focus" the array, we adopted a procedure whereby the fields of the individual apertures were selected to have a phase such that all contributions at the internal field point were additive. Now we could have turned the problem around and started with a hypothetical electric line source at the internal point and deduce the corresponding re-

ceived signal in each aperture. This would lead to an alternative but equivalent procedure to deduce the phase angles δ_n needed to design the focused aperture. This latter approach could be adapted to more complicated target geometries where purely numerical methods would be required to solve the electromagnetic problem. However, in the interim, it would seem prudent to restrict attention to analytically viable models if insight and understanding are desired. We are currently undertaking such a study and the results will be reported in Part II.

ACKNOWLEDGMENT

The author wishes to thank Dr. T. C. Cetas for his encouragement and support of this study.

REFERENCES

- [1] N. Morita and J. B. Andersen, "Near-field absorption in a circular cylinder from electric and magnetic line sources," *Bioelectromagnetics*, vol. 3, pp. 253-274, 1982.
- [2] J. R. Oleson, T. C. Cetas, and P. M. Cory, "Hyperthermia by magnetic induction: Experimental and theoretical results for coaxial coil pairs," *Radiation Res.*, vol. 96, pp. 175-186, 1983.
- [3] P. F. Turner, "Regional hyperthermia with an annular phased array," *IEEE Trans. Bio-Med. Eng.*, vol. BME-31, pp. 106-114, 1984.
- [4] G. Arcangeli, P. P. Lombardini, G. A. Lovisolo, G. Marsiglia, and M. Piattelli, "Focussing of 915 MHz electromagnetic power on deep human tissues," *IEEE Trans. Bio-Med. Eng.*, vol. BME-31, pp. 47-52, 1984.
- [5] W. Gee, S. W. Lee, N. K. Bong, C. A. Cain, R. Mittra, and R. L. Magin, "Focussed array hyperthermia applicator," *IEEE Trans. Bio-Med. Eng.*, vol. BME-31, pp. 38-46, 1984.
- [6] J. R. Oleson, "A review of magnetic induction methods for hyperthermia treatment of cancer," *IEEE Trans. Bio-Med. Eng.*, vol. BME-31, pp. 91-97, 1984.
- [7] J. R. Wait, *Electromagnetic Radiation from Cylindrical Structures*. London: Pergamon, 1959.
- [8] J. R. Wait, *Electromagnetic Wave Theory*. New York: Harper and Row, 1984.
- [9] M. Abramowitz and I. Stegun, *Handbook of Mathematical Functions*. New York: Dover, 1975.
- [10] H. S. Ho, A. W. Guy, R. A. Sigelmann, and J. F. Lehmann, "Microwave heating of simulated limbs by aperture sources," *IEEE Trans. Microwave Theory Tech.*, vol. MTT-19, pp. 224-231, 1971.
- [11] J. R. Wait and D. A. Hill, "Excitation of a homogeneous conductive cylinder of finite length by a prescribed current distribution," *Radio Sci.*, vol. 8, pp. 1169-1176, 1973.

Convergence of Local and Average Values in Three-Dimensional Moment-Method Solutions

MARK J. HAGMANN, MEMBER, IEEE, AND RONALD L. LEVIN

Abstract — Block models using 8, 64, 216, 512, 1000, 1728, and 2744 cubical cells were used to evaluate the local and average specific absorption rate (SAR) for a dielectric cube irradiated by an EM plane wave. All seven models were used in examples for 0.5-cm and 2.5-cm saline cubes at 400 MHz and a 30-cm cube of biological tissue at 27.12 MHz. In each example, the solutions using 8 or 64 cells were similar to that for a sphere rather than a cube. Many cells are needed to approximate the sharp variation of the electric field near corners and edges of a dielectric cube.

The heterogeneity of the electric field in an object having corners and edges causes a frequency-independent error (FIE) in addition to the more

Manuscript received October 9, 1984; revised February 25, 1985.

The authors are with the Biomedical Engineering and Instrumentation Branch, Division of Research Services, National Institutes of Health, 13/3W13, Bethesda, MD 20205.